Optimization of Chitosan Na-TPP Nanoparticle Formation from Parijoto Fruit Extract (*Medinilla speciosa*) using the Ionic Gelation Method

Optimization of Chitosan Na-TPP Nanoparticle Formation from Parijoto Fruit Extract *(Medinilla speciosa)* using the Ionic Gelation Method

Yohanes Alan Sarsita Putra[1*], Devi Chan Wai Han[1], Alberta Rika Pratwi[1], Bernadeta Soedarini[1], Ratna Shintia Defi[2], Victoria Kristina Ananingsih[1]

[1]Department of Food Technology and Innovation, Faculty Agricultural Technology, Soegijapranata Catholic University Jl. Rm. Hadisoebeno Sosro Wardoyo, Jatibarang, Kec. Mijen, Kota Semarang, Jawa Tengah, Indonesia
[2]Department of Medicine Science, Soegijapranata Catholic University Jl. Rm. Hadisoebeno Sosro Wardoyo, Jatibarang, Kec. Mijen, Kota Semarang, Jawa Tengah, Indonesia

[*]E-mail: alan@unika.ac.id

Abstract. Nanotechnology, exemplified by Chitosan Na-TPP nanoparticle (CNPs), employs ionic gelation to enhance the stability of chitosan polymer compounds. CNPs, non-toxic and facile to prepare, safeguard active compounds from degradation. This research investigated the physicochemical characteristics of Chitosan Nanoparticles formulated with parijoto extract, aiming to enhance the stability of anthocyanins in the *Medinilla speciosa* plant. Chitosan Nanoparticles (CNPs), synthesized through ionic gelation with *tripolyphosphate* (TPP) as a stabilizer, provided a method to overcome the inherent instability of anthocyanins. Chitosan concentrations of 0.8 g/cc, 1.6 g/cc, and 2.4 g/cc, along with 3%, 6%, and 9% parijoto extract solutions, were systematically explored to optimize nanoparticle formation. Zetasizer Pro analysis revealed key physicochemical parameters such as zeta potential, conductivity, particle size, and polydispersity index. Statistical analyses using the Response Surface Methodology, including lack of suitability tests, regression tests, and estimated influence tests, demonstrated a significant correlation between chitosan concentration, parijoto extract concentration, and the physicochemical characteristics of the nanoparticles. The optimal concentrations for chitosan, NaTPP and parijoto extract are 2.4 g/cc, 0.25 g/cc, and 7.5%, respectively, with a desirability value of 0.49, also categorized as moderate. The statistical analysis highlighted particle size and polydispersity index as variables with a significant correlation with chitosan and parijoto extract concentrations. These findings contribute valuable insights into the development of stable CNPs for potential applications in preserving bioactive compounds in parijoto fruit.

1. Introduction

Indonesia is recognized for its diverse flora, boasting over 30,000 plant species, including 7,000 medicinal herbs. Among these, the parijoto plant *(Medinilla speciosa)* stands out for its scientific benefits. Parijoto fruit, flourishing on the slopes of Mount Muria in the village of Colo, Dawe district, Kudus regency, Central Java, possesses a tangy taste and firm texture, with its reddish-

purple hue attributed to anthocyanin pigments [1,2]. Anthocyanins, soluble in water, imbue fruits and vegetables with blue, purple, orange, and red colours, functioning as antioxidants to combat free radicals and contributing to overall health. Parijoto fruit, rich in phenols, anthocyanins, flavonoids, and tannins, also harbours antioxidants [3].

Nanotechnology, exemplified by Chitosan nanoparticles, employs ionic gelation to enhance the stability of chitosan polymer compounds. Chitosan nanoparticles, non-toxic and facile to prepare, safeguard active compounds from degradation. Nano-sized food materials are pivotal in developing diverse nanostructures applicable to food, pharmaceuticals, and nutraceuticals [4]. Control over particle size distribution, concentration, and interfacial layer characteristics is achievable through adjustments in CNPs. Stabilization of nanoparticles becomes imperative to counteract their tendency to aggregate, especially when dealing with sizeable molecular surface areas and high surface energies. Utilizing tripolyphosphate (TPP) as a stabilizer, [5] successfully modified surfaces by combining chitosan and TPP, resulting in stable nanoparticles. Hydrogels, such as TPP, offer opportunities for formulating carriers with controllable geometry, positive surface charges, and efficient encapsulation capacities.

Chitosan, a linear cationic natural polymer, is a promising choice for polymer nanoparticle formation due to its commendable biocompatibility, biodegradability, adsorption properties, non-toxicity, and mucoadhesive capabilities [6]. The enhancement of chitosan gelation and cross-linking abilities, along with nanoparticle characteristics favouring small, uniform sizes and the use of cross-linking agents like tripolyphosphate plays a crucial role in this process. However, TPP is acknowledged as a flocculant that concurrently binds two particles, causing aggregation by bridging particles, leading to aggregation mechanisms during chitosan nanoparticle formation. Nadia et al. [7] asserted that adding TPP at the appropriate concentration, along with surfactants, strengthens the mechanical properties of brittle chitosan and facilitates the formation of ionic bonds between ions and chitosan molecules.

Anthocyanins are inherently unstable and prone to degradation due to various factors, including chemical structure, concentration, solvent, pH, storage temperature, light, proteins, and flavonoids. Demonstrating stability in solvents, Cruz et al. [8] illustrated that synthetic flavylium salt solutions in protic and aprotic solvents exhibited red and yellow colours, respectively. This colour variation arose from the formation of highly unstable monomer and dimer anthocyanins, susceptible to monomer loss, degradation, and colour changes under high pH, temperature, and light. It was reported that lower pH values correlate with higher anthocyanin stability. Ko et al.'s [9] research further indicated that heating at 35°C resulted in a 50% reduction in grape anthocyanin content compared to the temperature of 25°C.

Several studies on CNPs anthocyanin particles in food materials have been implemented. Chatterjee et al. [10] reported that black carrots contain anthocyanins suitable for nanoparticle formation. The optimal nanoencapsulation process yielded spherical nanoparticles with high encapsulation efficiency, enhancing in vivo anthocyanin antioxidant activity and signifying improved stability and bioavailability. Bulatao et al. [11] also stated that chitosan-alginate nanoparticles can effectively encapsulate anthocyanins derived from black glutinous rice. Ko et al.'s [9] research highlighted that nanoencapsulation combined with pigmentation is an effective technique to enhance black soybean anthocyanins' color and antioxidant properties. However, no study has been conducted on CNPs anthocyanin particles using parijoto fruit. This study aims to formulate Chitosan Na-TPP nanoparticles (CNPs) with the addition of parijoto extract, which is rich in anthocyanin content. The primary objectives of this study are threefold. Firstly, the physicochemical characteristics of CNP particles during their formation should be investigated,

mainly focusing on the impact of adding Parijoto extract and varying concentrations of chitosan. Secondly, to establish the optimal concentrations of Parijoto extract and chitosan that yield the most favorable conditions for forming CNPs particles. Lastly, identifying the optimum formulation parameters that lead to the successful formation of CNPs with Parijoto extract aims to contribute valuable insights into developing effective CNPs formulations.

2. Material And Methods

2.1 Materials

Fresh parijoto, ethanol pro analysis (Merck, Germany), methanol pro analysis (Merck, Germany), distilled water, aqua bikes, folding ciocalteu 10% (Merck, Germany), Na_2CO_3 7.5% (Merck, Germany), DPPH solution (Merck, Germany), Quarcetin (Merck, Germany), $AlCl_3$ (Merck, Germany), ammonium acetate 1 M (Merck, Germany), acetone (Merck, Germany), acetonitrile (Merck, Germany), standard cyanide (Zigma), delphinidin glu standard (Zigma), Chitosan (Merck, Germany).

2.2 Experimental Design

This study followed an experimental design in the form of a Design Experiment of Response Surface Methodology. Chitosan, combined with the stabilizer NaTPP and the incorporation of parijoto extract, served as the samples. The comprehensive research design for formulating CNPs particles with the addition of parijoto extract is depicted in the flowchart below. In this study, the production of CNPs particles with the addition of parijoto extract was undertaken. The variables utilized in this research included dependent variables, namely the concentration of chitosan and parijoto extract. Meanwhile, the independent variables consisted of the zeta potential, conductivity, pH, viscosity, particle size, and polydispersity index of the CNPs. Each variable was measured through three repetitions, and measurements were repeated three times to obtain consistent results. The repetitions of the tests can be observed in Table 1.

Table 1. Independent Variable Chitosan Nanoparticles Formation Of Parijoto Fruit Extract

Symbol	Independent Variable	Code Levels		
		-1 (Low)	**0 (Middle)**	**+ 1 (High)**
$\mathbf{X_1}$	Chitosan Concentration (g/cc)	0.8	1.6	2.4
$\mathbf{X_2}$	Parijoto Extract Concentration	3	6	9

2.3 Preparation Of Chitosan Acetate Solution Chitosan Nanoparticle Particles

Using a digital balance, the chitosan acetate solution was prepared by weighing Smart Lab brand chitosan powder at 0.8 g, 1.6 g, and 2.4 g. Subsequently, 400 ml of 1% acetic acid was weighed. The chitosan powder was mixed with 1% acetic acid and heated to 50°C at 300 rpm for 1 hour until fully dissolved on a magnetic stirrer. The Na-TPP solution was prepared by mixing NaTPP powder with aquabides. Before this, 0.1 g of NaTPP powder was weighed. Then, NaTPP was dissolved in IKA brand aquabides at 100 ml on a magnetic stirrer at 30°C for 30 minutes at 300 rpm. The preparation of the parijoto extract solution began with heating the parijoto extract to

30°C to obtain a liquid texture from its initially thick state. The parijoto extract was then filtered using 0.2 μm filter paper and dissolved in aquabides with concentration variations of 3%, 6%, and 9%, totalling 375 ml. A Na-TPP solution containing 0.1 g/cc was mixed with parijoto extract at different concentrations. Each mixture underwent three repetitions. Creating the parijoto extract Na-TPP mixture took 30 minutes at 30°C at 300 rpm on a magnetic stirrer. The homogenous parijoto extract Na-TPP solution was then gradually mixed with chitosan acetate drop by drop for each concentration. The dissolution was repeated at 40°C for 1 hour on a magnetic stirrer. Subsequently, the solution was checked using a pH meter, and NaOH was added dropwise until reaching a pH of 5.8 to 6. The solution was homogenized again for 15 minutes on a magnetic stirrer.

2.4 Characterization Of Particle Size And Polydispersity Index Of Chitosan Nanoparticles Parijoto Fruit Extract

The particle size analysis tool used in this study was the, which operates based on the general principle of dynamic light scattering. This tool has a detector placed at an angle of 173° from the transmitted light beam and detects size using a patented technology known as noninvasive backscattering. This technique is used for various purposes. One is to reduce the effect known as multiple scattering, making it easier to measure samples with high concentrations. Modifying McClements [12], the particle size distribution and average particle size of nanoparticles were determined by dynamic light scattering (DLS) at a wavelength of 633 nm and a temperature of 25 °C.

2.5 Characterization Of ζ-potential and Conductivity Chitosan Nanoparticles Parijoto Fruit Extract

The ζ-potential of the samples was evaluated automatically using 10 to 100 analytical runs after equilibration for 120 s at 25 °C. The ζ-potential of the particles was measured by phase-analysis light scattering using a Zeta dip cell. The conductivity of nanoemulsion and chitosan nanoparticles was measured by phase-analysis light scattering (PLS) using a Zeta dip cell with a cuvet electrode. Samples were evaluated automatically using 10 to 100 analytical runs after equilibration for 120 seconds at 25 °C. The detector is placed at an angle of 173° from the transmitted light beam.

2.6 pH Measurement Of Chitosan Nanoparticles Parijoto Fruit Extract

The pH was determined using a Schott pH meter at room temperature (27 ± 2 °C), calibrated with a standard buffer of pH 7. The pH analysis of the Parijoto fruit extract nanoemulsion sample was carried out using a pH meter with a special electrode. First, the pH meter is set and calibrated with a standard buffer solution at a known pH, generally at pH 4.0, 7.0, and 10.0. Samples were diluted with 10 mM phosphate buffer pH seven before analysis, to avoid multiple scattering effects during testing. The pH meter electrode is then carefully inserted into the sample to ensure good contact. Once the electrode is stable, a pH reading is taken and recorded. This step is repeated as necessary to obtain consistent results. This pH analysis provides important information regarding the acidity or alkalinity level of CNPs Parijoto fruit extract, which can affect the stability and quality of products using the chitosan nanoparticles.

2.7 Viscosity Measurement Of Chitosan Nanoparticles Parijoto Fruit Extract

Viscosity measurements are carried out using a viscometer instrument. 14 mL of sample was put into the cup and attached to the solvent trap provided. The viscometer was set at 200 rpm, three rotations, for 30 seconds. The measurement process begins by activating the viscometer, and this

tool automatically measures the time required for a liquid to flow through the viscometer tube at a specific temperature and rpm. This time, a predetermined formula converts the reading into a viscosity value. Repeated measurements can be made to ensure consistent results.

2.8 Data Analysis Using Response Surface Method

In this study, primary data were gathered through three repetitions of extraction, and the average test data, along with standard deviation values for each treatment combination, were presented based on three replications. The obtained data analysis using the Statistica program, employing a combination of factorial points, axial points, and central points, with each test repeated three times. The variability in standard deviation sample values introduced additional uncertainty into the calculated values, posing challenges in determining the probability distribution of each studied statistic. The study utilized a Central Composite Design (CCD) model. The effect summary test encapsulates the combined treatment effects, represented by log-worth values derived from -log (p-value) transformations based on the Pearson Chi-Squared test. Higher Pearson Chi-Squared values indicate an increased likelihood of splits due to dependence. A log worth more significant than 2 suggests statistical significance in the model.

The Lack of Fit test aimed to determine the model's suitability for predicting the response. The hypotheses were established and concluded by comparing calculated and tabulated F-values. If the calculated F-value < tabulated F-value, the model was deemed suitable. On the other hand, the Summary of Fit test utilized R-square and Root Mean Square Error (RMSE) values to assess the model's predictive accuracy. Parameter estimates, representing the change in response with specific predictor levels, were derived, akin to multiple regression analysis. The Analysis of Variance (ANOVA) test determined the model's statistical acceptance based on F-values. The quadratic model equation was expressed as

$$y = interface + X1 + X2 + X1^2 + X2^2 + X1.X2.$$

The study employed the CCD model for the fitted surface representation. CCD, chosen over the Box-Behnken Design, offered more design points and the ability to explore extreme values. It contained full factorial or fractional factorial designs and axial points, allowing for curvature estimation. The study emphasized the advantages of CCD, including its ability to run experiments at extreme values and provide a better quadratic equation for analysis.

3. Result And Discussion

3.1 Characterization of Particle Size and Polydispersity of Chitosan Nanoparticles Parijoto Fruit Extract

Table 2. presents the results of particle size characterization and polydispersity of parijoto fruit extract CNPs for each sample tested. Particle size is measured in nanometers, and the polydispersity index describes the degree to which the particle size distribution is homogeneous or heterogeneous. These data are important for assessing the stability and quality of nanoparticles. The smaller the particle size and the closer to zero the polydispersity value is, the more homogeneous the distribution.

Table 2. Particle Characterization and Polydispersity Index of Chitosan Nanoparticles Parijoto Fruit Extract

No	Sample Code	Particle Size (nm)	*Polydispersity Index* (PDI)
1	CNP A 1	319.433 ±8.329	0.572 ± 0.094
2	CNP A 2	438.200 ±9.337	0.763 ± 0.064
3	CNP A 3	454.867±16.737	0.703 ± 0.066
4	CNP B 1	417.600 ±16.690	0.751 ± 0.137
5	CNP B 2	441.100 ±9.007	0.802 ± 0.171
6	CNP B 3	687.500 ±3.897	0.578 ± 0.019
7	CNP C 1	570.200 ±11.625	0.593 ± 0.066
8	CNP C 2	743.900 ±14.625	0.798 ± 0.138
9	CNP C 3	1138.233±7.606	0.883 ± 0.125

Note: The values displayed are the mean and standard deviation (n=3).

The formation of CNPs through the ionic gelation method was easily achieved due to the complexation between positively and negatively charged components during mechanical stirring. This separated chitosan into spherical particles with varying sizes and surface charges. Nanoparticle characterization included particle size, polydispersity, zeta potential, conductivity, pH, and viscosity. Chitosan nanoparticle particle sizes generally range from 20 to 200 nm and 550 to 900 nm [13]. This aligns with Table 2, indicating an average CNPs particle size of 319.433 nm to 1,138.233 nm. Bashir et al. [14] supported this, stating that anion particles diffusing into chitosan molecules and causing crosslinking would result in nanoparticle sizes ranging from 200 to 1,000 nm. The molecular weight and degree of acetylation of chitosan significantly influenced particle size and surface charge. Solution properties, including polymer and acid concentrations in the solvent, could also contribute to variations. Stirring time was another factor linked to increased particle size due to potential agglomeration during the procedure [14,15].

Nanoparticle size distribution was expressed through the Polydispersity Index (PDI). PDI is used to estimate the average uniformity of particle solutions, with higher PDI values indicating a more significant size distribution in the particle sample [16]. In Table 2, CNPs with Parijoto fruit extract had PDI values ranging from 0.572 to 0.883, indicating a very high size distribution. Systems with PDI values <0.1 are considered highly monodisperse, while values > 0.4 and those in the range of 0.1 to 0.4 indicate moderately dispersed polydispersive systems [17]. Some PDI results from this study fell into the moderately dispersed category. The ionic gelation method produces particles susceptible to aggregate or agglomerate formation, especially at higher chitosan concentrations, longer stirring times, and higher stirring speeds. These conditions may lead to flocculation or coagulation phenomena, resulting in non-uniform particle sizes and reducing colloidal stability. Jha et al. [18] reported that using the ionic gelation method had difficulty achieving uniform nanoparticle production. Stirring time is another factor related to increased particle size because particles can agglomerate during this procedure [18]. This method allows for over-gelation or over-crosslinking due to excessive stirring time and speed, leading to massive particles or agglomerates due to excess cross-reactions. Factors such as high stirring speed cause poor hydrodynamic conditions during the nanoparticle formation, leading to aggregate formation [15]. Factors like time and stirring speed in the ionic gelation method also result in low mechanical stability.

3.2 Characterization of Z-potential and Conductivity of Chitosan Nanoparticles Parijoto Fruit Extract

Table 3. presents the results of the ζ-potential and conductivity characterization of Parijoto fruit extract CNPs. Z-potential is measured in millivolts (mV) and describes the surface charge of colloidal particles. Positive or negative values indicate charge polarity, while zero values indicate neutrality. Conductivity is measured in milli Siemens per centimetre (mS/cm) and reflects the ability of a liquid to conduct electric current.

Table 3. Characterization of Z-potential and Conductivity of Chitosan Nanoparticles Parijoto Fruit Extract

No	Sample Code	ζ -potential (mV)	Conductivity (mS/cm)
1	CNP A 1	-22.893 ± 0.574	0.063 ± 0.002
2	CNP A 2	-21.526 ± 0.704	0.064 ± 0.001
3	CNP A 3	-22.076 ± 1.190	0.064 ± 0.009
4	CNP B 1	-23.703 ± 2.186	0.069 ± 0.004
5	CNP B 2	-23.746 ± 1.251	0.068 ± 0.010
6	CNP B 3	-24.533 ± 1.001	0.071 ± 0.009
7	CNP C 1	-22.78 ± 1.383	0.070 ± 0.008
8	CNP C 2	-23.927 ± 1.328	0.063 ± 0.001
9	CNP C 3	-22.293 ± 1.050	0.070 ± 0.001

Note: The values displayed are the mean and standard deviation (n=3).

The quality of nanoparticle outcomes was determined by zeta potential. Z-potential represents the electric charge between colloidal particle surfaces. A higher ζ-potential value inhibits flocculation. According to H K Ardani et al. [17], Z-potential values indicate the colloid stability of formed nanoparticles in a solution. Table 3 shows a ζ-potential value range of -24.533 to -21.526, signifying a sufficiently high zeta potential, suggesting the stability of the resulting colloid. The negative values obtained were influenced by acetic acid, resulting in a negative charge. This charge causes repulsive forces between formed nanoparticles, preventing aggregation into larger sizes. Z-potential values within ± 0-10 mV indicate highly unstable colloids, ±10-20 mV, ±20-30 mV, and > ±30 mV indicate relatively stable, moderately stable, and highly stable colloids, respectively. Particles with significantly positive or negative ζ-potential values create repulsive forces between particles, while low positive or negative ζ-potential values cause attractive forces, leading to instability. In cases of combined electrostatic and steric stabilization, utilizing NaTPP as a stabilizer in this study through ionic gelation, the desired minimum ζ-potential is ±20 mV. Particles should have ζ-potential variance >10 mV for more excellent stability [18]. The expected range for ζ-potential values is -30 mV to 20 mV or +20 mV to +30 mV.

Conductivity indicates the ability of a substance to conduct free ions present in a solution. Table 3 shows conductivity values ranging from 0.063 mS/cm to 0.071 mS/cm. Minea et al. [19] stated that the range of electrical conductivity is between 0.001 mS/cm and 0.005 mS/cm, which means the conductivity values in Table 2 are below this data. Decreasing conductivity values can occur due to the formation of neutral ion pairs when the distance between dissociated ions becomes less. This happens due to the aggregation of non-moving ion species.

3.3 Characterization of pH and Viscosity of Chitosan Nanoparticles Parijoto Fruit Extract

Table 4 includes the pH and viscosity characterization results of Parijoto fruit extract CNPs. pH measures a solution's acidity or alkalinity level, while viscosity measures the thickness of a liquid. These data are important for evaluating the stability and applicability of CNPs in the context of product formulation. An appropriate pH can support the stability and availability of active compounds in the extract. In contrast, an appropriate viscosity can influence the flow properties and application of products using this nanoemulsion.

Table 4. Characterization of pH and Viscosity of Chitosan Nanoparticles Parijoto Fruit Extract

No	Sample Code	pH	Viscosity (Cp)
1	CNP A 1	5.946 ± 0.055	3.810 ± 0.010
2	CNP A 2	5.926 ± 0.025	3.840± 0.010
3	CNP A 3	5.973 ± 0.050	3.880 ± 0.010
4	CNP B 1	5.923 ± 0.015	3.930 ± 0.010
5	CNP B 2	5.940 ± 0.026	3.973 ± 0.005
6	CNP B 3	6.016 ± 0.005	3.970 ± 0.010
7	CNP C 1	5.953 ± 0.049	4.100 ±0.010
8	CNP C 2	5.926 ± 0.005	4.200 ± 0.010
9	CNP C 3	5.983 ± 0.055	4.433 ± 0.057

Note: The values displayed are the mean and standard deviation (n=3).

The formation of CNPs is also influenced by pH. Chitosan and its stabilizer, sodium tripolyphosphate (NaTPP), are pH-dependent components, meaning pH can affect the ionic interactions in forming CNPs. Table 4 shows the average acidity level obtained from CNPs ranging from 5.923 to 6.016. Chitosan has a pH of around 6.5 [20]. Meanwhile, Warsito et al. [21] stated that chitosan TPP nanoparticles would have a pH range of 1.9 to 7.5. Viscosity is one of the parameters used to determine polymer stability in a solution because of reductions during polymer storage due to polymer degradation [22]. In this study, as seen in Table 4, the viscosity of CNPs ranged from 3.810 cp to 4.433 cp. Alemu et al. [23] researched that viscosity can depend on particle size and storage time. CNPs have lower viscosity, around 30%, compared to a normal chitosan solution with the same concentration. Storage time can also decrease normal chitosan viscosity by about 10% over 24 hours, while nanoparticle viscosity decreases by 17% over the same storage period.

3.5 Fitting for Response Surface Methodology on Parijoto Fruit Extract Chitosan Nanoparticles

Data recorded for each run included CNPs particle size, polydispersity index, ζ-potential, conductivity, pH, and viscosity. This data will be used to analyze the influence of various factors on the characteristics of nanoparticles using the Response Surface Methodology method, which can be seen in the Table 5.

The fitting table is important for evaluating the statistical significance of each model component and determining whether or not the quadratic model used is good enough to explain the characteristics of the nanoemulsion. The p-value is used to determine statistical significance, and the analysis results will help select an appropriate model and interpret the significance of factors that influence the characteristics of nanoparticles, which can be seen in the Table 6.

Table 5. Design Of Experiment Chitosan Nanoparticles Formation Of Parijoto Fruit Extract

		Independent Variable				Dependent Variable			
No. Run Test	**Sample Code**	**Chitosan Concentration (g/cc)**	**Parijoto Extract Concentration**	**Particle Size (nm)**	**Zeta Potential (mV)**	**Conductivity (mS/cm)**	**Polydispersity Index**	**pH**	**Viskositas (Cp)**
		X1	**X2**	**Y1**	**Y2**	**Y3**	**Y4**	**Y5**	**Y6**
1	CNP A 1	0.8	3	3	325.3	-23.24	0.4906	3.832	5.92
2	CNP A 1	0.8	6	3	323.1	-23.21	0.5507	3.984	6.01
3	CNP A 1	0.8	9	3	309.9	-22.23	0.6762	3.734	5.91
4	CNP A 2	0.8	3	6	442.4	-21.12	0.745	3.879	5.93
5	CNP A 2	0.8	6	6	444.7	-22.34	0.8349	3.981	5.9
6	CNP A 2	0.8	9	6	427.5	-21.12	0.7108	3.778	5.95
7	CNP A 3	0.8	3	9	473.1	-21.45	0.7787	4.342	6.02
8	CNP A 3	0.8	6	9	451.3	-21.33	0.6788	3.245	5.92
9	CNP A 3	0.8	9	9	440.2	-23.45	0.6528	4.123	5.98
10	CNP B 1	1.6	3	3	402	-24.55	844.4	4.392	5.91
11	CNP B 1	1.6	6	3	415.6	-25.34	0.5932	3.928	5.92
12	CNP B 1	1.6	9	3	435.2	-21.22	0.8178	4.353	5.94
13	CNP B 2	1.6	3	6	447.5	-23.45	1	3.987	5.97
14	CNP B 2	1.6	6	6	430.8	-25.12	0.7131	4.849	5.93
15	CNP B 2	1.6	9	6	445	-22.67	0.6932	3.543	5.92
16	CNP B 3	1.6	3	9	685.2	-24.15	0.5619	4.945	6.02
17	CNP B 3	1.6	6	9	692	-23.78	0.5736	3.859	6.01
18	CNP B 3	1.6	9	9	685.3	-25.67	0.5999	4.112	6.02
19	CNP C 1	2.4	3	3	583.6	-24.33	0.6016	3.785	6.01
20	CNP C 1	2.4	6	3	562.8	-21.67	0.5232	4.278	5.92
21	CNP C 1	2.4	9	3	564.2	-22.34	0.6553	4.764	5.93
22	CNP C 2	2.4	3	6	728.8	-25.46	0.7073	3.829	5.93
23	CNP C 2	2.4	6	6	744.9	-23.11	0.729	3.748	5.93
24	CNP C 2	2.4	9	6	758	-23.21	0.9579	3.893	5.92
25	CNP C 3	2.4	3	9	1145	-22.12	0.7505	4.283	6.01
26	CNP C 3	2.4	6	9	1130	-23.42	0.899	4.375	6.02
27	CNP C 3	2.4	9	9	1139.7	-21.34	1	4.234	5.92

Table 6. Fitting Table for RSM Quadratic Model Particle Size, Poly Dispersity Index, Zeta Potential, Conductivity, pH, Viscosity in Chitosan nanoparticles

Quadratic Model Equation	Sources of Variation	p-Value
Particle Size (R^2 : 0.666 R^2_a : 0.644)	Model	0.000*
$Y = 285.358 + 101.6217X_1 + 84.3654X_2 + 24.65 X_1^2 - 20.744 X_2^2 + 26.3043X_1X_2$	*Lack of fit*	0.270
Poly Dispersity Index (R^2 : 0.049 R^2_a : 0.0)	Model	0.037
$Y = 7.5095 + 0.0111 X_1 - 11.3446 X_2 - 22.661 X_1^2 - 11.2513 X_2^2 - 0.0674 X_1X_2$	*Lack of fit*	0.876
Z-potential (R^2 : 0.273 R^2_a : 0.224)	Model	0.000*
$Y = 7.5095 + 0.0111 X_1 - 11.3446 X_2 - 22.661 X_1^2 - 11.2513 X_2^2 - 0.0674 X_1X_2$	*Lack of fit*	0.269
Conductivity (R^2 : 0.274 R^2_a : 0.225)	Model	0.000*
$Y = -0.39244 - 0.01299 X_1 + 0.004266 X_2 - 0.045222 X_1^2 - 0.006 X_2^2 + 0.000981X_1X_2$	*Lack of fit*	0.885
pH (R^2 : 0.423 R^2_a : 0.00)	Model	0.000*
$Y = 5.682367 + 0.010095 X_1 + 0.027933 X_2 + 0.010103 X_1^2 + 0.024365 X_2^2 - 0.00891 X_1X_2$	*Lack of fit*	0.481
Viscocity (R^2 : 0.073 R^2_a : 0.011)	Model	0.002*
$Y = 4.01601 + 2.73652 X_1 + 0.17302 X_2 + 2.26541 X_1^2 - 3.66028 X_2^2 + 0.13603 X_1X_2$	*Lack of fit*	0.290

Notes : *: The model has a statistically significant effect (p≤0.05); **: Model mismatch or lack of fit occurs (p≤0.05)

Based on the ANOVA results of 3 concentration factors and Parijoto fruit extract, most probability values showed figures (p<0.05), meaning some data were significant. This indicates that the response surface quadratic model used for both responses is significant and can be used to optimize extraction factors. In the summary table of the fit results for concentration factors and Parijoto fruit extract, the R^2 of the regression model for particle size reached 0.66635 nm. The polydispersity index regression model reached 0.04991, the ζ-potential regression model reached 0.27308, the conductivity regression model reached 0.27407, the pH regression model reached 0.04298, and the viscosity regression model reached 0.07357. These results indicate that several regression models are significant and adequate in describing the data distribution [24].

The coefficient of determination R-square reflects how well independent data can explain dependent data, and values are obtained between 0 and 1. The closer to 1, the better, and if the R-square is 0.6, the independent variable can explain 60% of the variation in the dependent variable. In comparison, the remaining 40% may be caused by other variables outside the independent variable as a limitation regarding model reliability. In the Central Composite Design analysis, the p-value indicates the significance of coefficients in the constructed polynomial regression model. The lower the p-value, the more significant the coefficients are to the overall regression model. Although some coefficients are insignificant, some experts argue that these coefficients remain relevant and should be retained in the overall regression model [25].

3.6 3D plot on Particle Size, Poly Dispersity Index, Zeta Potential, Conductivity, pH, and Viscosity as a function of Chitosan Nanoparticles Parijoto Fruit Extract.

In this research, the model is created as a Contour plot, which can show the response, which in this case is Particle Size, Polydispersity Index, Zeta Potential, Conductivity, pH, and Viscosity. The surface plot above illustrates the predicted values for particle size (Figure 1. a). The average particle size is plotted against the concentration of Parijoto Fruit Extract in the range of 3-9%. The graph displays the surface plot for the particle size of Parijoto fruit extract CNPs, with the lower prediction limit for total concentration in the range <190 nm and the upper limit in the range >400 nm. The surface plot above indicates the predicted values for particle size. Polydispersity is plotted against the concentration of Parijoto Fruit Extract in the range of 3-9%. The image shows the surface plot for the polydispersity of Parijoto fruit extract CNPs, with the lower prediction limit for total polyphenol concentration in the range <-10 and the upper limit in the range >20 (Figure 1. b).

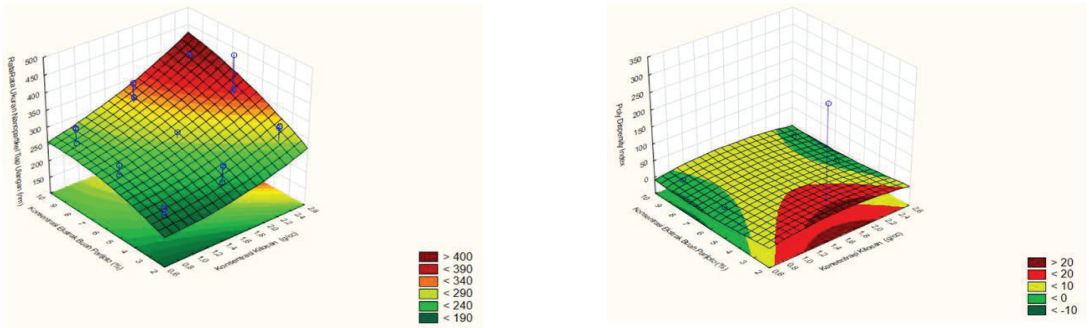

Figure 1. 3D Plot as a function of Chitosan Nanoparticles Parijoto Fruit Extract (a. Particle Size & b. Polydispersity Index).

One of the independent variables used is the concentration of chitosan with three treatment levels, namely 0.8 g/cc, 1.6 g/cc, and 2.4 g/cc. In Tables 2, 3, and 4, an increasing trend can be observed in particle size, PDI, and viscosity, but for pH, zeta potential, and conductivity, there is no significant increase with increasing concentration. Ahmad et al. [26] reported that higher chitosan concentrations lead to the formation of larger particle sizes in CNPs. The study reported that CNPs particle size increased from 150 nm to 195 nm when the initial chitosan concentration was increased from 0.05 w/v to 0.3% w/v. Excessive chitosan concentration leads to an excess cross-linking process between chitosan and TPP, occurring rapidly, and CNPs tend to aggregate and form larger particle sizes.

Increasing the concentration of chitosan resulted in the production of larger CNPs particles due to the greater participation of chitosan in the particle formation process, influencing its molecular interactions. The elevated chitosan concentration enhanced these interactions and affected the particle structure, forming longer polymer chains of chitosan. Particle size increased with the rise in chitosan concentration, but the ζ-potential of these CNPs particles was not significantly affected by chitosan concentration [27]. Based on the results obtained, particle size and viscosity increased with the increase in chitosan concentration. Smaller particle sizes were achieved with lower chitosan concentrations and vice versa. The smaller particle size directly influenced the reduction in the viscosity of the chitosan solution. The chitosan solution should have good solubility for a more efficient gelation process. If the chitosan concentration exceeds the limit, nano-particles will begin to aggregate and form larger particles.

On the contrary, Lin et al. [28] found that higher concentrations of chitosan were unsuitable for CNPs formation due to unacceptable polydispersity indices and large nanoparticle sizes resulting from flocculation due to excess chitosan in the system. Higher chitosan concentrations significantly increased particle size, which is related to the aggregation or agglomeration process at higher chitosan concentrations. Optimal CNPs, where the PDI value reaches the lowest, indicate a more homogeneous particle size distribution.

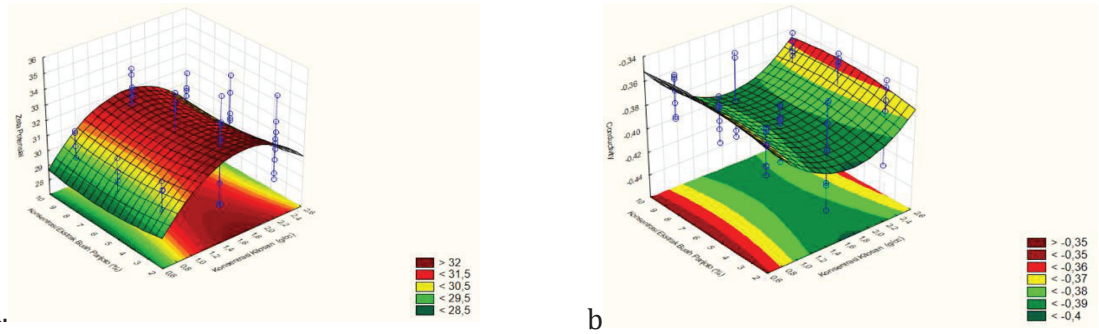

a. b

Figure 2. 3D Plot as a function of Chitosan Nanoparticles Parijoto Fruit Extract (a. Z-potential & b. Conductivity).

The surface plot above illustrates the predicted values for ζ-potential (Figure 2. a). Z-potential is plotted against the concentration of Parijoto Fruit Extract in the range of 3-9%. The graph shows the surface plot for the ζ-potential of Parijoto fruit extract CNPs, with the upper prediction limit for the size level in the range >32 mV and the lower limit <28.5 mV. Conductivity against the concentration of Parijoto Fruit Extract in the range of 3-9% (Figure 2. b). The image shows the surface plot for the conductivity of Parijoto fruit extract CNPs, with the upper prediction limit for the size level in the range >-0.35 mS/cm and the lower limit <-0.4 mS/cm. In this study, one of the manipulated independent factors was the concentration level of Parijoto fruit extract as a filler material for nano-particles, consisting of three treatment levels: 3%, 6%, and 9%. The results obtained only showed an increase in the particle size and viscosity of Parijoto fruit extract CNPs. In other aspects of the profile, no significant relationship was observed with the increase in the extract. The solvent used was water, which is highly suitable for various bioactive compound extractions contained in Medinilla sp. Using aquabides could produce a purer extract, especially if Parijoto fruit has soluble compounds. This aids in obtaining a more consistent extract free from solvent contaminants.

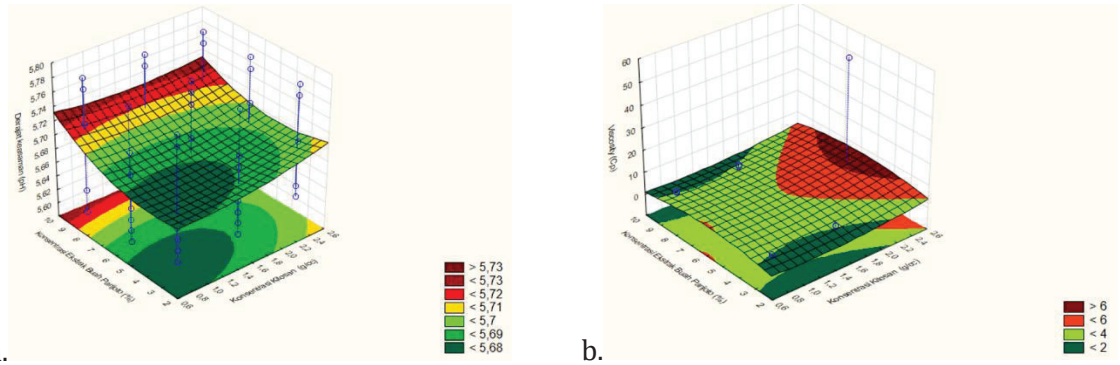

a. b.

Figure 3. 3D Plot as a function of Chitosan Nanoparticles Parijoto Fruit Extract (a. pH & b. Viscosity).

pH is plotted against the concentration of Parijoto Fruit Extract in the range of 3-9%. Total chitosan concentration is plotted against the concentration of NaTPP in the range of 5.68 – 5.73. The surface plot above shows the predicted viscosity values. Viscosity concentration is plotted against the concentration of Parijoto Fruit Extract in the range of 3-9%. The image illustrates the surface plot for viscosity, with the upper prediction limit for the size level in the range >6 Cp and the lower limit for viscosity <2 Cp. Increasing the concentration of a specific filler extract can cause CNPs to tend to aggregate or form agglomerates. This can occur if there are physical or chemical interactions between CNPs particles and substances in the filler extract. Ananingsih et al. [29] stated the same, noting that when increasing the extract concentration, the particle size of the sample increased significantly, reaching (347.2). Meanwhile, the smallest concentration ratio reported the smallest size with a (86.98) nm value. This indicates that at higher concentrations, the likelihood of particle agglomeration may increase.

The increase in Parijoto fruit extract concentration can add total mass to the solution, increasing viscosity in general. Additional particles or molecules from the filler extract can contribute to increased viscosity. CNPs produced with the highest concentration obtained the highest viscosity and vice versa. This increase is caused by an excess load of the extract in chitosan particles. The filler extract may have specific physicochemical characteristics that influence the viscosity properties of CNPs. Changes in pH, temperature, or chemical composition can affect viscosity enhancement.

3.7 Optimal Point Prediction from RSM in Chitosan Nanoparticles Parijoto Fruit Extract

Optimal point predictions from the Response Surface Methodology are obtained by combining optimal conditions based on interactions between independent variables. Profiler predictions are obtained if the fitted surface graph is in minimum, maximum, or saddle form. 3D graphics on Figure 4 shows a complex interaction between the variable factors of lipophilic tween type and tween concentration on the response. There is an optimal region where the response reaches its peak. The implication for practice is that by setting the variable factors at levels that are estimated to be optimum, the research results and CNPs can achieve the highest optimization in the desired response, which can be seen in Figure 4.

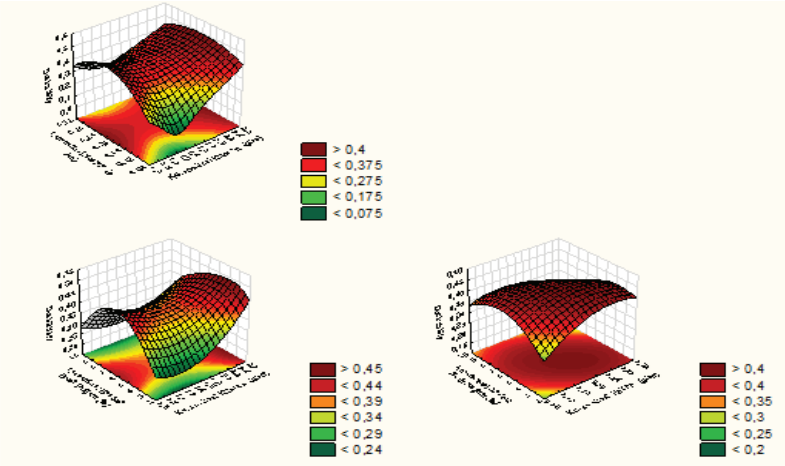

Figure 4. Profile Graphs and 3D Desirability Response of Chitosan Nanoparticles Parijoto Fruit Extract.

Table 7. Prediction Of Optimum Conditions For Parijoto Fruit Extract Chitosan Nanoparticles

Types of Analysis	Chitosan Concentration	NaTPP concentration	Parijoto Fruit Extract Concentration (%)	Nanoparticle Size (nm)	Z-potential (mV)	Conductivity (mS/cm)	Poly Dispersity Index	pH	Viscosity (Cp)	Desirability Value
Optimum Condition Prediction	2.4	0.25	7.5	395.75	30.52	-0.36	0.8360	5.7	7.1	0.49
Maximum value at optimal conditions	2.4	0.25	7.5	397	31.5	-0.41	0.1107	5.73	10.27	
Minimum value at optimal conditions	2.4	0.25	7.5	394.5	29.53	-0.32	0.9779	5.67	3.93	

In Table 7, it can be seen that to achieve the maximum desired values of nanoparticle size, zeta potential, Conductivity, Polydispersity Index, degree of acidity, and Viscosity, the chitosan concentration must be adjusted to 2.4 g/cc, the NaTPP concentration to 0.25 g /cc, and the concentration of parijoto fruit extract to around 7.5%. This combination of conditions gives a desirability value of 0.4954. This value is categorized as moderate. In Table 7, to achieve the desired concentrations of nanoparticle size, zeta potential, conductivity, polydispersity index, acidity, and viscosity, the chitosan concentration needs to be set at 2.4 g/cc and the Parijoto fruit extract concentration at 7.5%. This set of conditions has a desirability value of 0.498. Because the value is not close to 1 and falls into the moderate category, a moderate desirability value, for example, between 0.5 and 0.8, can be used to determine optimal conditions, considering the importance of each response variable [30].

Figure 4 depicts surface plots for the particle size of Parijoto fruit extract CNPs with the lower prediction limit for total concentration in <190 nm and the upper limit in the range >400 nm. The surface plot for the polydispersity of Parijoto fruit extract CNPs shows the lower prediction limit for total polyphenol concentration in the range <-10 and the upper limit in the range >20. The surface plot for the ζ-potential is >-32 mV with the lower limit <-28.5 mV. Figure 4 also presents a surface plot for conductivity at >-0.35 mS/cm, with the lower limit <-0.4 mS/cm. The total chitosan concentration is plotted against NaTPP concentration in the range 5.68 – 5.73. The surface plot for viscosity is >6 Cp, with the lower limit for viscosity <4 Cp. The prediction of optimal points from the Response Surface Methodology is obtained by combining optimal conditions based on the interaction between independent variables [31]. The prediction profiler is obtained when the fitted surface graph is in a minimum, maximum, or saddle shape. The optimization process will achieve optimal response results from analyzing each previous response and can minimize effort and operational costs. A higher desirability value approaching 1 indicates a higher level of suitability for the combination of process parameters used to obtain the expected optimal response variable combination [32].

4. Conclusion

In conclusion, the increased concentrations of chitosan and parijoto extract significantly influence the physical characteristics, particle size, and polydispersity of chitosan nanoparticles. Elevated chitosan concentration leads to the formation of longer polymer chains, potentially resulting in aggregation during excessive concentrations, thereby affecting particle size and polydispersity index. The characterization of chitosan nanoparticles reveals a ζ-potential ranging from -24.533 to -21.526 mV, polydispersity index values ranging from 0.572 to 0.883, particle sizes ranging from 319.433 to 1138.233 nm, conductivity ranging from 0.063 to 0.071 mS/cm, pH ranging from 5.923 to 6.016, and viscosity ranging from 3.810 to 4.433 cp. The optimal concentrations determined are 2.4% for chitosan and 7.5% for parijoto extract, yielding a desirability value of 0.49, indicating a moderate outcome.

Acknowledgements

The authors would like to express their sincere gratitude to the LPPM SCU for their invaluable funding support, which made this research possible. Their generous contribution has significantly contributed to the success of this study. During the preparation of this work, the authors used Grammarly to improve readability and language. After using this program, the authors reviewed the content of the publication.

References

[1] Ananingsih VK, Pratiwi AR, Soedarini B, Putra YA. Formulation of nanoemulsion parijoto fruit extract (Medinilla speciosa) with variation of tweens stabilizers. Front Nutr. 2024 Jul 8;11:1398809.
[2] Defi RS, Putra YA, Asmara GY, Ananingsih VK. Eksplorasi Potensi Tanaman Tropis Indonesia sebagai Bahan Alami Anti-Aging Kulit: Analisis Fitokimia dan Aktivitas Antioksidan. Damianus J Med. 2025 Aug 31;24(2):134–46.
[3] Ananingsih VK, Marcellino CA, Sakoco KF, Putri NI, Soedarini B, Pratiwi Putra YA, Setiawan FB. Physical and Chemical Stability of Parijoto Fruit Extract (Medinilla speciosa) Nanodispersion in different pH Solutions. Curr Res Nutr Food Sci. 2025 Aug 1;13(2).
[4] Magne TM, Alencar LMR, Carneiro SV, Fechine LMUD, Fechine PBA, Souza PFN, et al. Nano-Nutraceuticals for Health: Principles and Applications. Rev Bras Farmacogn. 2023;33(1):73–88. doi:10.1007/s43450-022-00338-7 .
[5] Juliantoni Y, Hajrin W, Subaidah WA. Nanoparticle Formula Optimization of Juwet Seeds Extract (Syzygium cumini) using Simplex Lattice Design Method. J Biol Tropis. 2020;20(3):416–22. doi:10.29303/jbt.v20i3.2124.
[6] Nunes R, Serra AS, Simaite A, Sousa Â. Modulation of Chitosan-TPP Nanoparticle Properties for Plasmid DNA Vaccines Delivery. Polymers. 2022;14(7):1443. doi:10.3390/polym14071443.
[7] Nadia LMH, Suptijah P, Ibrahim B. Production and Characterization Chitosan Nano from Black Tiger Shrimp with Ionic Gelation Methods. J Pengolahan Hasil Perikanan Indones. 2014;17(2):119–26. doi:10.17844/jphpi.v17i2.8700.
[8] Luis Cruz N, Basílio N, Mateus N, de Freitas V, Pina F. Natural and Synthetic Flavylium-Based Dyes: The Chemistry Behind The color. Chem Rev. 2022;122(1):1416–81. doi:10.1021/acs.chemrev.1c00399.
[9] Ko A, Lee JS, Nam HS, Lee HG. Stabilization of black soybean anthocyanin by chitosan nanoencapsulation and copigmentation. J Food Biochem. 2017;41(2):e12316. doi:10.1111/jfbc.12316.
[10] Chatterjee NS, Dara PK, Perumcherry Raman S, Vijayan DK, Sadasivam J, Mathew S, et al. Nanoencapsulation in low-molecular-weight chitosan improves in vivo antioxidant potential of black carrot anthocyanin. J Sci Food Agric. 2021;101(12):5264–71. doi:10.1002/jsfa.11175.
[11] Bulatao RM, Samin JPA, Salazar JR, Monserate JJ. Encapsulation of anthocyanins from black rice (Oryza sativa L.) bran extract using chitosan-alginate nanoparticles. J Food Res. 2017;6(3):40–7. doi:10.5539/jfr.v6n3p40.
[12] McClements DJ. Food emulsions: principles, practices, and techniques. CRC Press; 2016.
[13] Mohammed MA, Syeda JT, Wasan KM, Wasan EK. An overview of chitosan nanoparticles and its application in non-parenteral drug delivery. Pharmaceutics. 2017;9(4):53. doi:10.3390/pharmaceutics9040053.
[14] Bashir O, Bhat SA, Basharat A, Qamar M, Qamar SA, Bilal M, et al. Nano-engineered materials for sensing food pollutants: Technological advancements and safety issues. Chemosphere. 2022;292:133320. doi:10.1016/j.chemosphere.2021.133320.
[15] Zhu HJ, Liu XM, Yang H, Shen XD. Effect of the stirring rate on physical and electrochemical properties of LiMnPO4 nanoplates prepared in a polyol process. Asian J Pharm Sci. 2014;9(5):252-7. doi:10.1016/j.ajps.2014.09.005.
[16] Clayton KN, Salameh JW, Wereley ST, Kinzer-Ursem TL. Physical Characterization of Nanoparticle Size and Surface Modification Using Particle Scattering Diffusometry. Biomicrofluidics. 2016;10(5):054107. doi:10.1063/1.4962992.
[17] Ardani HK, Imawan C, Handayani W, Djuhana D, Harmoko A, Fauzia V. Enhancement of the stability of silver nanoparticles synthesized using aqueous extract of Diospyros discolor Willd. leaves using polyvinyl alcohol. IOP Conf Ser Mater Sci Eng. 2017;188(1):012056. doi:10.1088/1757-899X/188/1/012056.
[18] Jha R, Mayanovic RA. A Review of the Preparation, Characterization, and Applications of Chitosan Nanoparticles in Nanomedicine. Nanomaterials. 2023;13(8):1302. doi:10.3390/nano13081302.
[19] Oudih Samar B. Chitosan Nanoparticle with controlled size and zeta potential. Polym Eng Sci. 2023;63(3):1011–21.
[20] Minea AA, Moldoveanu GM, Huminic G, Huminic A. Al2O3/TiO2 hybrid nanofluids thermal conductivity. J Therm Anal Calorim. 2019;137:583–92. doi:10.1007/s10973-018-7974-4.
[21] Karimi N, Ghanbarzadeh B, Hajibonabi F, Hojabri Z, Ganbarov K, Kafil HS, et al. Turmeric Extract Loaded Nanoliposome as A Potential Antioxidant and Antimicrobial Nanocarrier for Food Applications. Food Biosci. 2019;29:110–7. doi:10.1016/j.fbio.2019.04.006.
[22] Warsito M, Agustiani F. A review on factors affecting chitosan nanoparticles formation. IOP Conf Ser Mater Sci Eng. 2021;1011:012027. doi:10.1088/1757-899X/1011/1/012027.
[23] Aranaz I, Alcántara AR, Civera MC, Arias C, Elorza B, Heras Caballero A, et al. Chitosan: An Overview of Its Properties and Applications. Polymers. 2021;13(19):3256. doi:10.3390/polym13193256.
[24] Alemu D, Getachew E, Mondal AK. Study on the Physicochemical Properties of Chitosan and their Applications in the Biomedical Sector. Int J Polym Sci. 2023;2023. doi:10.1155/2023/5025341.

[25] Liu Z, Wang C, Hou J, Wang P, Miao L, Lv B, et al. Aggregation, sedimentation, and dissolution of CuO and ZnO nanoparticles in five waters. Environ Sci Pollut Res Int. 2018;25(31):31240–9. doi:10.1007/s11356-018-3123-7.
[26] Anderson MJ, Whitcomb PJ. RSM Simplified. Boca Raton: CRC Press; 2017.
[27] Ahmad A, Mubarak NM, Naseem K, Tabassum H, Rizwan M, Najda A, et al. Recent advancement and development of chitin and chitosan-based nanocomposite for drug delivery: Critical approach to clinical research. Arab J Chem. 2020;13(12):8935–64. doi:10.1016/j.arabjc.2020.10.019.
[28] Lin P, Moore D, Allhoff F. What is nanotechnology and why does it matter?: from science to ethics. John Wiley & Sons; 2009.
[29] Ananingsih VK, Pratiwi AR, Soedarini B, Putra YA. Teknologi Nanoemulsi dan Nanokitosan Ekstrak Antosianin Buah Parijoto (Medinilla speciosa). Unika Publisher. 2023.
[30] Morales-Olán G, Luna-Suárez S, Figueroa-Cárdenas JDD, Corea M, Rojas-López M. Synthesis and characterization of chitosan particles loaded with antioxidants extracted from chia (Salvia hispanica L.) seeds. Int J Anal Chem. 2021;2021. doi:10.1155/2021/5540543.
[31] Bezerra MA, Santelli RE, Oliveira EP, Villar LS, Escaleira LA. Response surface methodology (RSM) as a tool for optimization in analytical chemistry. Talanta. 2008;76(5):965–77. doi:10.1016/j.talanta.2008.05.019.
[32] Ananingsih VK, Soedarini B, Andriani C, Konstantia BA, Santoso BD. Optimization of encapsulated agents and stirring speed on the physicochemical characteristics of vacuum dried nutmeg seed oleoresin (Myristica fragrans). J Food Process Preserv. 2022 Dec;46(12):e17151. doi:10.1111/jfpp.17151.